Symmetry and Symmetry Breaking in Electrostatic MEMS

*J.A. Pelesko, **D.H. Bernstein, and †J. McCuan

* Univ. of Delaware, Dept. of Mathematical Sciences, Newark, DE, 19716, pelesko@math.udel.edu
** Consultant, MEMS and Microelectronics, Berkeley, CA, 94707, dhbernstein@earthlink.net
† Georgia Inst. of Tech. School of Mathematics, Atlanta, GA, 30332, mccuan@math.gatech.edu

ABSTRACT

The use of electrostatic forces to provide actuation is a method of central importance in microelectromechanical systems (MEMS) and is of growing importance in nanoelectromechanical systems (NEMS). The study of electrostatic actuation has led to numerous interesting experimental, theoretical, and numerical results. Yet, surprisingly, even simple electrostatically actuated systems have secrets to reveal. Here, we study the electrostatic deflection of an annular elastic membrane. We consider the so-called small aspect ratio approximate model of electrostatically deflected membranes. We ask whether or not solutions to this model automatically inherit the symmetry of the annular domain. Through a numerical investigation we show that in fact, asymmetric solutions exist. That is, there is a symmetry breaking bifurcation present in this model for the electrostatically deflected annular system.

Keywords: electrostatic actuation, pull-in, instability, semi-linear elliptic problem, symmetry breaking

1 Introduction

In 1968, in the context of investigating fundamental questions in electrohydrodynamics, G.I. Taylor studied the electrostatic deflection of elastic membranes [1]. Utilizing a soap film as the membrane material and applying a fixed high voltage potential difference between two supported circular membranes, Taylor showed experimentally that at a critical voltage the two membranes snap together and touch. The equilibrium state where the membranes remained separate that existed at smaller voltages either became unstable or failed to exist. This instability is familiar to researchers in the MEMS and NEMS fields where it is known as the "pull-in" instability. In fact, in an interesting historical coincidence H.C. Nathanson [2] and his coworkers studied this instability in the context of a primitive MEMS device at roughly the same time as Taylor was conducting his studies. Nathanson is responsible for the "pull-in" nomenclature and the analysis of a mass-spring model of this effect. Taylor, in conjunction with R.C. Ackerberg [3], developed and numerically analyzed a more accurate membrane based model of electrostatic deflection. Recently, a rigorous analysis of this model was completed [4]. Surprisingly, even on circular domains, and using this simplified model, one finds a rich solution set exhibiting a bifurcation diagram with infinitely many folds. Nonetheless, all solutions in this case are rotationally symmetric; they inherit the symmetry of the circular boundary. In this paper, we consider whether or not this statement is true in the general case. We consider the system shown in Figure 1 and ask whether electrostatically deflected membranes always inherit the symmetry properties of the membrane's domain. Are asymmetric deflections possible? This study is partially motivated by examples of other physical systems similar to the electrostatic membrane system that undergo symmetry breaking bifurcations. One of the most dramatic can be found in the work of Rhode [5]. Rhode studied annular surfaces of constant mean curvature. These surfaces minimize surface area subject to a volume constraint. Physically, this system is realized by an annular soap film formed over a common "Bundt" pan. The soap film attempts to minimize its area, but must enclose the volume of air between the film and the Bundt pan. This volume can be varied by blowing air into the Bundt pan through a small connected tube. Like the electrostatic system of Figure 1 when Ω is an annulus, the Rhode system is an example of a nonlinear boundary value problem on a symmetric domain. Surprisingly, as the volume of air in the Bundt pan is increased the so-

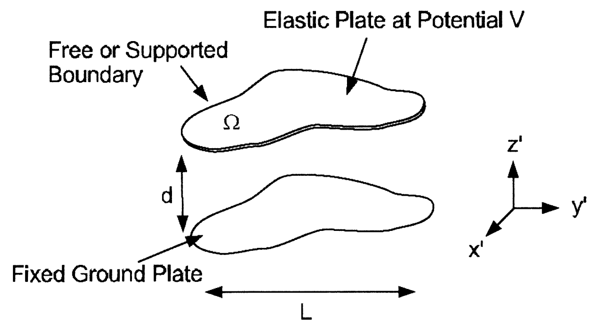

Figure 1: A basic electrostatically actuated elastic membrane. The primed coordinates indicate that they have not been scaled.

Figure 2: The Rhode experiment after symmetry breaking.

lutions to this highly symmetric problem become asymmetric. A symmetry breaking bifurcation occurs. The Bundt pan experiment is easy to carry out, a picture of an asymmetric solution is shown in Figure 2. While the Rhode system bears a striking resemblance to the electrostatic system, we should keep in mind the differences. In particular, in the Rhode model the nonlinearity arises as a consequence of the term representing mean curvature. As we shall explore below, in the small aspect ratio electrostatic model the mean curvature term has been linearized and the nonlinearity arises as a consequence of the nonlinear Coulomb force.

2 The Mathematical Model

Referring to Figure 1 we review the small aspect ratio approximate model of electrostatically deflected elastic membranes. This model has been studied extensively. We refer the reader to [6] for a more detailed discussion of the formulation and further references. In Figure 1 we assume the electrostatic potential satisfies Laplace's equation everywhere away from the two plates and appropriate boundary conditions on the plates. In dimensionless form these equations may be written as

$$\delta^2\left(\frac{\partial^2\psi}{\partial x^2}+\frac{\partial^2\psi}{\partial y^2}\right)+\frac{\partial^2\psi}{\partial z^2}=0, \qquad (1)$$

$$\psi=0 \text{ on ground plate}, \qquad (2)$$

$$\psi=1 \text{ on membrane}, \qquad (3)$$

where ψ is a dimensionless potential scaled with respect to the source voltage, V, x and y are scaled with respect to the length of the undeformed plate, z is a vertical coordinate scaled with respect to the undeformed gap size, and δ is an aspect ratio of the device, i.e., the ratio of the undeformed gap size to the device length. The displacement, u, is assumed to satisfy

$$\triangle u=\lambda\left[\delta^2\left(\left(\frac{\partial\psi}{\partial x}\right)^2+\left(\frac{\partial\psi}{\partial y}\right)^2\right)+\left(\frac{\partial\psi}{\partial z}\right)^2\right], \qquad (4)$$

$$u=0 \text{ on boundary}, \qquad (5)$$

where we have assumed that u has been scaled in the same manner as z. Here $\lambda=\epsilon_0V^2L^2/2Tl^3$, where l is undeflected gap size, L is a length scale of the membrane, T is the tension the membrane is under, and ϵ_0 is the permittivity of free space. Note that λ characterizes the relative strengths of electrostatic and mechanical forces in the problem. Next, we simplify our governing equations by assuming that the aspect ratio, δ, is small. Accordingly, we send δ to zero, solve the resulting simplified potential equation and use this approximate potential in the elastic equation. The upshot of this analysis is that the problem can be reduced to the following semi-linear elliptic equation for the displacement

$$\triangle u=\frac{\lambda}{(1+u)^2} \qquad (6)$$

with the boundary conditions given by equation (5).

3 Detection of Symmetry Breaking

Axially symmetric solutions of equations (5) and (6) on an annular domain satisfy the ordinary differential equation

$$\frac{d^2u}{dr^2}+\frac{1}{r}\frac{du}{dr}=\frac{\lambda}{(1+u)^2} \qquad (7)$$

with boundary conditions

$$u(\epsilon)=u(1)=0. \qquad (8)$$

Here, ϵ is a dimensionless ratio of the inner and outer annulus radii (thus $0<\epsilon<1$). Numerical shooting was used to solve this boundary value problem and to construct the bifurcation diagram for various values of ϵ. The case $\epsilon=0.1$ is shown in Figure 3. Possible symmetry breaking bifurcation points can be located by seeking a solution to equations (5) and (6) of the form

$$u(r,\theta)=u^*(r)+\gamma v(r,\theta)+O(\gamma^2) \qquad (9)$$

where $u^*(r)$ is a numerically computed axially symmetric solution and γ is a small deviation from the axially symmetric branch of solutions. Ignoring terms of $O(\gamma^2)$ yields a linear problem for v. Separating variables reduces the problem to a linear variable coefficient eigenvalue problem. The variable coefficient depends on $u^*(r)$. If this eigenvalue problem has a solution then a likely bifurcation point has been detected. This eigenvalue problem was solved numerically to detect such points. The first detected possible bifurcation point for the case $\epsilon=0.1$ is shown in Figure 3.

4 Computing Asymmetric Solutions

We seek solutions to

$$\frac{\partial^2u}{\partial r^2}+\frac{1}{r}\frac{\partial u}{\partial r}+\frac{1}{r^2}\frac{\partial^2u}{\partial\theta^2}=\frac{\lambda}{(1+u)^2} \qquad (10)$$

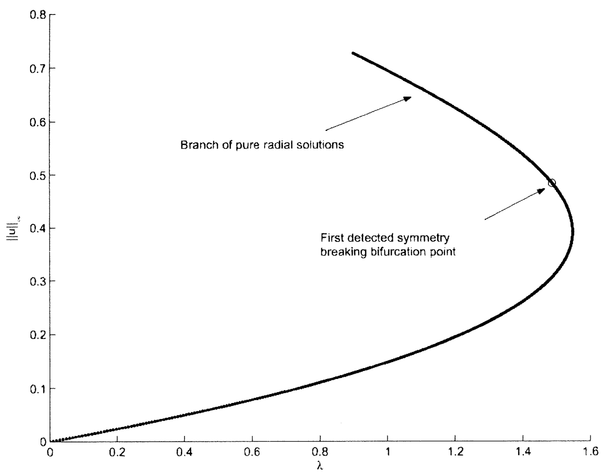

Figure 3: Numerically computed bifurcation diagram showing the location of a possible symmetry breaking bifurcation. The ordinate is the maximum deflection of the membrane. $\epsilon = 0.1$ for for this family of solutions.

on the annular domain discussed above with boundary conditions (8). Note that (10) is invariant under transformations of the form $\theta \to \theta + \phi$, so that if there is one symmetry breaking solution there is an infinite number of them. We eliminate this symmetry by imposing a Neumann condition at $\theta = 0, \pi$:

$$\frac{\partial u}{\partial \theta}(0) = \frac{\partial u}{\partial \theta}(\pi) = 0. \tag{11}$$

Note that this condition is restrictive: there may be non-axially symmetric solutions which do not satisfy it. If so, the code which we describe in this section will not find them.

We attempt to numerically approximate solutions using the method of finite differences on an evenly spaced grid given by

$$r_i = i\left(\frac{1-\epsilon}{N+1}\right) + \epsilon, \quad \theta_j = \frac{\pi(j-1)}{M-1}, \tag{12}$$

where $i = 1 \ldots N$ and $j = 1 \ldots M$. Substituting the standard second order finite difference approximations for the derivatives in (10) results an a coupled set of nonlinear algebraic equations for the solution vector $u_{i,j}$. This system can be solved using the well-known Newton-Raphson algorithm (see for instance [9]).

To follow solutions along branches which have intersections and folds we use the arclength continuation method developed by Keller and coworkers (e.g., [7], [8]). In this method we add a new parameter, s, to the system so that now λ and $u_{i,j}$ are functions of s. Let s_k be a value of s at which we have a solution $u(s_k)$, $\lambda(s_k)$. Then the pseudo-arclength equation is

$$\dot{u}(s_k)\cdot(u(s)-u(s_k))+\dot{\lambda}(\lambda(s)-\lambda(s_k))-(s-s_k) = 0 \tag{13}$$

where the dot denotes the derivative with respect to s and $u \cdot u$ is a suitably defined inner product for u.

The starting point is the solution $u = 0$ at $\lambda = 0$. In this case we can choose $s_0 = 0$ and begin the arclength computation at this point. For a given s_k we use the linear approximation

$$\dot{\lambda} \approx \frac{\lambda(s_k) - \lambda(s_{k-1})}{s_k - s_{k-1}} \tag{14}$$

and similarly for $\dot{u}$. Hence given $\lambda(s_k)$ and $u(s_k)$ we solve the entire system consisting of the discretized form of (10) and (13) to get the solution at s_{k+1}.

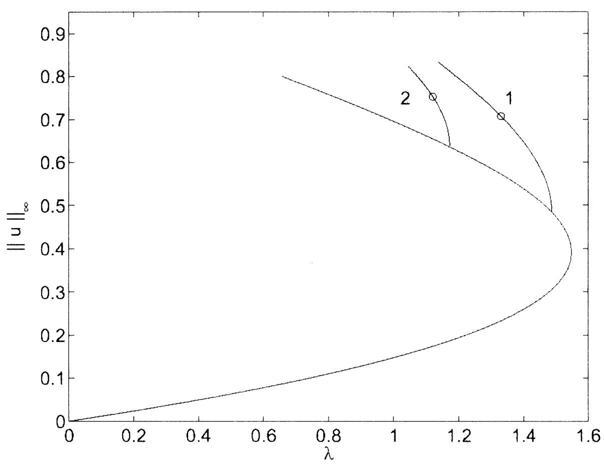

Figure 4: Computed bifurcation diagram for the case $\epsilon = 0.1$. The ordinate is the maximum deflection of the membrane. The circle marked "1" is the location of the single minimum solution plotted in Figure 5 while the circle marked "2" corresponds to the solution in Figure 6.

As is shown in [7], [8], points where branches of the solution intersect occur when the Jacobian of the full system becomes singular. For the case of two branches intersecting, the null space of the Jacobian at this point is one dimensional and the null vector is simply the tangent vector of the other branch. This makes switching branches a simple matter of detecting when the Jacobian becomes singular and using the null vector to move onto the other branch. Numerically, the method we use is to perform a singular value decomposition of the Jacobian at each step of the arclength algorithm. When the smallest singular value drops below a given tolerance, the code attempts to find a solution in the direction of the vector associated with this singular value. While this method is far from foolproof it seems to work well in this application.

Figure 4 shows part of the bifurcation diagram of the problem (10), (8), and (11) which has been computed in this manner. For the figures in this section we have set $\epsilon = 0.1$, $N = 40$, and $M = 40$. There are two additional branches intersecting the axially symmetric branch. The left branch consists of solutions having one minimum while the right branch solutions have two minima. Representative solutions are shown in Figures 5 and 6 respectively. Note that the intersection point of the left branch agrees approximately with that computed in the previous section using the linearized eigenvalue problem.

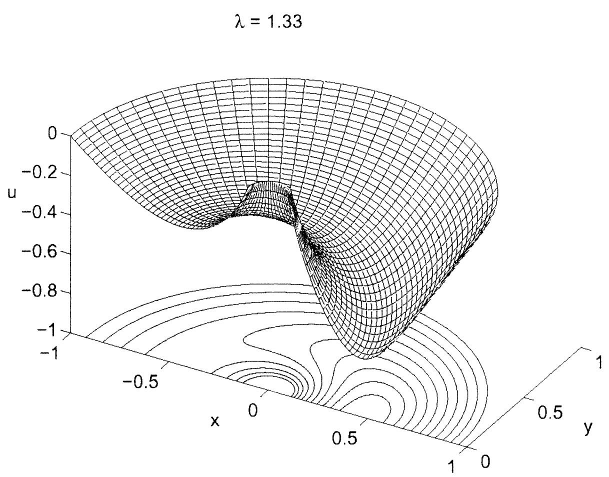

Figure 5: An asymmetric solution with one minimum. This solution occurs at the point marked "1" in Figure 4.

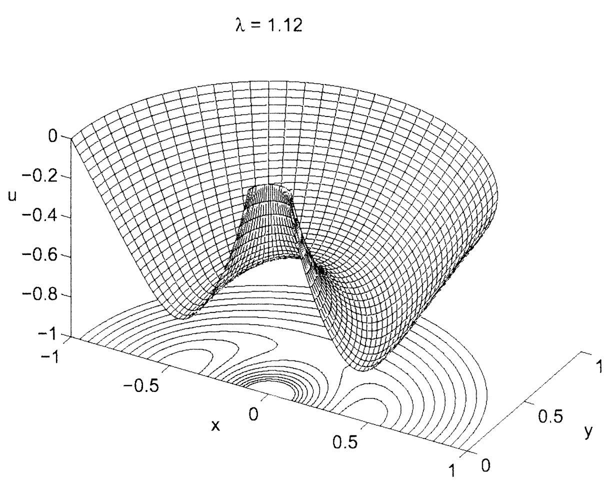

Figure 6: An asymmetric solution with two minima. This solution occurs at the point marked "2" in Figure 4.

5 Discussion

The bifurcation diagram and the nature of the nonsymmetric solutions suggests that there are an infinite number of branches intersecting the upper axially symmetric branch, each distinguished by the number of minima of the deflection. As in other investigations of electrostatically deflected membranes with folds, we expect the solutions on the upper branch, including the nonsymmetric branches, to be dynamically unstable. We expect that stable electrostatically deflected films (observed experimentally) are, in fact, rotationally symmetric; the nonsymmetric solutions considered in this paper should be of significance only in the unstable regime. Preliminary experimental and numerical results agree with this expectation.

6 Acknowledgements

We thank Roberto Eduardo Lopez of the Georgia Institute of Technology for providing the picture of the Rhode experiment. D.B. thanks M. Tokman for letting him use the laptop with Matlab on it.

REFERENCES

[1] G.I. Taylor, *The Coalescence of Closely Spaced Drops when they are at Different Electric Potentials*, Proc. Roy. Soc. A, 306 (1968), pp. 423-434.

[2] H.C. Nathanson, W.E. Newell, R.A. Wickstrom and J.R. Davis, *The Resonant Gate Transistor*, IEEE Trans. on Electron Devices, 14 (1967), pp. 117-133.

[3] R.C. Ackerberg, *On a Nonlinear Differential Equation of Electrohydrodynamics*, Proc. Roy. Soc. A., 312 (1969), pp. 129-140.

[4] J.A. Pelesko and X.Y. Chen, *Electrostatically Deflected Circular Elastic Membranes*, Jrnl. of Electrostatics, in press.

[5] A.K. Rhode, *Rotation-Symmetric Surfaces of Constant Mean Curvature in Two Concentric Circles*, Dissertation, Universitat Bonn, Mathematisches Institut, 1996.

[6] J.A. Pelesko and D.H. Bernstein, *Modeling MEMS and NEMS*, Chapman Hall and CRC Press, (2002).

[7] E. Doedel, H.B. Keller, and J.P. Kernevez, *Numerical Analysis and Control of Bifurcation Problems, Part I*, Int. J. of Bifurcation and Chaos, 1 (1991), pp. 493-520.

[8] E. Doedel, H.B. Keller, and J.P. Kernevez, *Numerical Analysis and Control of Bifurcation Problems, Part II*, Int. J. of Bifurcation and Chaos, 1 (1991), pp. 745-772.

[9] W.H. Press, S.A. Teukolsky, W.T. Vetterling, and B.P. Flannery, *Numerical Recipes in C* (1993), Cambridge University Press, Cambridge.